Edited by Martin Bertau, Erik Mosekilde
and Hans V. Westerhoff

WILEY-VCH

Biosimulation in Drug Development

10
Optimizing Temporal Patterns of Anticancer Drug Delivery by Simulations of a Cell Cycle Automaton

Atilla Altinok, Francis Lévi, and Albert Goldbeter

Abstract

Determining the optimal temporal pattern of drug administration represents a central issue in chronopharmacology. Given that circadian rhythms profoundly affect the response to a variety of anticancer drugs, circadian chronotherapy is used clinically in cancer treatment. Assessing the relative cytotoxicity of various temporal patterns of administration of anticancer drugs requires a model for the cell cycle, since these drugs often target specific phases of this cycle. Here we use an automaton model to describe the transitions through the successive phases of the cell cycle. The model accounts for the progressive desynchronization of cells due to the variability in duration of the cell cycle phases, and for the entrainment of the cell cycle by the circadian clock. Focusing on the cytotoxic effect of 5-fluorouracil (5-FU), which kills cells exposed to this anticancer drug during the S phase, we compare the effect of continuous infusion of 5-FU with various circadian patterns of 5-FU administration that peak at either 4 a.m., 10 a.m., 4 p.m., or 10 p.m. The model indicates that the cytotoxic effect of 5-FU is minimum for a circadian delivery peaking at 4 a.m. – which is the profile used clinically for 5-FU – and is maximum for continuous infusion or a circadian pattern peaking at 4 p.m. These results are explained in terms of the relative temporal profiles of 5-FU and the fraction of cells in S phase.

10.1
Introduction

Multiple links exist between circadian rhythms and cancer. First, the rate of tumor growth in rodents increases as a result of: (a) mutations affecting the circadian clock [1] and (b) disruption of the neural pacemaker governing circadian rhythms [2]. Second, the cell cycle is directly controlled by the circadian clock [3–5]. This explains why progression through the cell cycle often displays a strong circadian dependence [6–9]. Third, the link between the circadian clock and cancer is further illustrated by the effect of circadian rhythms on a variety of anticancer medica-

Biosimulation in Drug Development. Edited by Martin Bertau, Erik Mosekilde, and Hans V. Westerhoff

ISBN: 978-3-527-31699-1

tions [10–12]. Each cancer medication is characterized, during the 24-h period, by a specific pattern of tolerance (chronotolerance) and efficacy (chronoefficacy) [12]. Moreover, the dosing time which results in the least toxicity of a drug for host cells usually achieves best antitumor efficacy [13]. The marked influence of circadian rhythms on chronotolerance and chronoefficacy has motivated the development of chronotherapeutic approaches, particularly in the field of cancer [10–15].

Assessing the effectiveness of various temporal schedules of drug delivery is central to cancer chronotherapeutics. Modeling tools can help to optimize time-patterned drug administration to increase effectiveness and reduce toxicity [16]. Probing the effect of circadian delivery of anticancer drugs by means of modeling and numerical simulations requires a model for the cell cycle. Different models for the cell cycle have been proposed. The complexity of these models increases as new molecular details are added [17–22]. Building on previous models for the embryonic and yeast cell cycles and for modules of the mammalian cycle [17–22], we are currently developing a model for the mammalian cell cycle in terms of a sequential activation of cyclin-dependent protein kinases, which behaves as a self-sustained biochemical oscillator in the presence of sufficient amounts of growth factors (C. Gérard and A. Goldbeter, in preparation). We have also developed a complementary, more pragmatic approach that shuns molecular details and relies on a simple phenomenological description of the cell cycle in terms of an automaton, which switches between sequential states corresponding to the successive phases of the cell cycle. In this model, the transition between some phases of the cell cycle, i.e. cell cycle progression or exit from the cycle, is affected by the presence of anticancer medications. The cell cycle automaton model is based on the perspective that the transitions between the various phases of the cell cycle entail a random component [23–25]; this model is directly inspired by our previous study of a follicular automaton model for the growth of human hair follicles [26, 27]. The model allows us to investigate how different temporal patterns of drug administration affect cell proliferation.

Anticancer medications generally exert their effect by interfering with the cell division cycle, often by blocking it at a specific phase. Thus, anticancer drugs exert most of their cytotoxicity on dividing cells through interactions with cell cycle or apoptosis-related targets [10–15]. Antimetabolites, such as 5-fluorouracil (5-FU), are primarily toxic to cells that are undergoing DNA synthesis, i.e. during the S-phase, while antimitotic agents, such as vinorelbine or docetaxel, are primarily toxic to cells that are undergoing mitosis, during the M phase. Conversely, alkylating agents such as cyclophosphamide or platinum complexes seldom display any cell cycle phase specificity. To illustrate the use of the cell cycle automaton model, we focus here on the chronotherapeutic scheduling of 5-FU, a reference drug for treating gastrointestinal, breast and various other cancers. The half-life of this medication is 10–20 min; thus, the exposure pattern is the only one considered here since it matches rather well the corresponding chronotherapeutic drug-delivery schedule [28].

A marked circadian dependence of the pharmacology of 5-FU has been demonstrated, both in experimental models and in cancer patients [29]. These data led

to the development of intuitive chronomodulated delivery schedules aiming to minimize the toxic effects of 5-FU on healthy cells through its nighttime, rather than daytime, infusion. The most widely used chronomodulated schedule of 5-FU involves the sinusoidal modulation of its delivery rate from 10 p.m. to 10 a.m., with a peak at 4 a.m., in diurnally active cancer patients (see Fig. 10.3b below). This scheme improves patient 5-FU tolerability up to five-fold as compared with constant-rate infusion and makes possible a 40% increase in the tolerable dose and the near-doubling of antitumor activity in patients with metastatic colorectal cancer [30, 31]. The 5-FU chronomodulated schedule with peak delivery at 4 a.m. proves to be much less toxic than other circadian schedules, in which peak delivery differs from 4 a.m. by 6–12 h [32].

In this chapter we resort to the automaton model for the cell cycle to investigate the comparative cytotoxicity of different chronomodulated schedules of 5-FU administration. The analysis brings to light the importance of the circadian time of the peak in 5-FU as well as the effect of the variability in cell cycle phase durations in determining the response to this antiproliferative drug. The results explain why the least toxic schedule of 5-FU delivery for diurnally active cancer patients is a circadian modulated drug-administration pattern that peaks at 4 a.m., and why the most cytotoxic drug-administration schedule is either a circadian pattern that peaks at 4 p.m. or a continuous infusion [33]. Modeling the case of 5-FU illustrates an approach that can readily be extended to other types of anticancer drugs acting upon different stages of the cell cycle.

10.2
An Automaton Model for the Cell Cycle

10.2.1
Rules of the Cell Cycle Automaton

The automaton model for the cell cycle (Fig. 10.1a) is based on the following assumptions:

1. The cell cycle consists of four successive phases along which the cell progresses: G1, S (DNA replication), G2, and M (mitosis).

2. Upon completion of the M phase, the cell transforms into two cells, which immediately enter a new cycle in G1 (the possibility of temporary arrest in a G0 phase is considered elsewhere).

3. Each phase is characterized by a mean duration D and a variability V. As soon as the prescribed duration of a given phase is reached, the transition to the next phase of the cell cycle occurs. The time at which the transition takes place varies in a random manner according to a distribution of durations of cell cycle phases. In the case of a uniform probability distribution, the duration varies in the interval $[D(1 - V), D(1 + V)]$.

4. At each time step in each phase of the cycle the cell has a certain probability to be marked for exiting the cycle and dying at the nearest G1/S or G2/M transition. To allow for homeostasis, which corresponds to the maintenance of the total cell number within a range in which it can oscillate, we further assume that cell death counterbalances cell replication at mitosis. Given that two cells in G1 are produced at each division cycle, the probability P_0 of exiting the cycle must be of the order of 50% over one cycle to achieve homeostasis. When the probability of exiting the cycle is slightly smaller or larger than the value yielding homeostasis, the total number of cells increases or decreases in time, respectively, unless the probability of quitting the cycle is regulated by the total cell number.

We use these rules to simulate the dynamic behavior of the cell cycle automaton in a variety of conditions. Table 10.1 lists the values assigned in the various figures to the cell cycle length, presence or absence of cell cycle entrainment by the circadian clock, initial conditions, variability of cell phase duration, and probability of quitting the cell cycle.

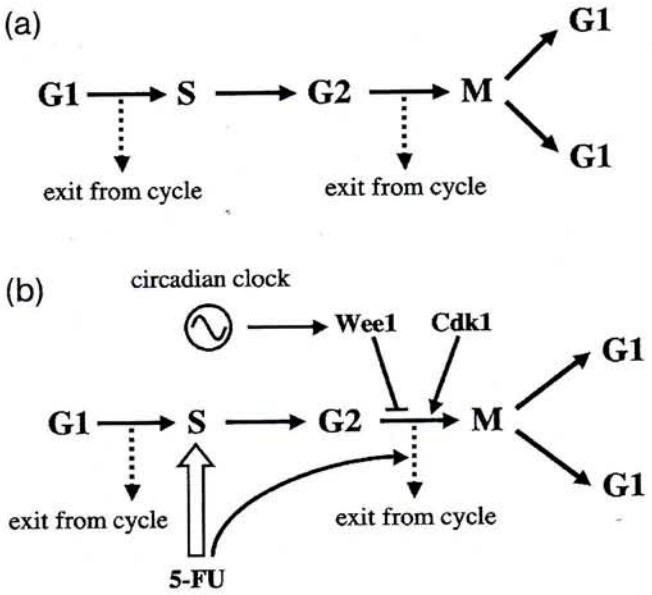

Fig. 10.1 (a) Scheme of the automaton model for the cell cycle. The automaton switches sequentially between the phases G1, S, G2, and M after which the automaton cell divides and two cells enter a new G1 phase. Switching from one phase to the next one occurs in a random manner as soon as the end of the preceding phase is reached, according to a transition probability related to a duration distribution centered for each phase around a mean value D and a variability V (see text). Exit from the cell cycle occurs with a given probability at the G1/S and G2/M transitions. (b) Coupling to the circadian clock occurs via the kinases Wee1 and cdc2 (Cdk1), which respectively inhibit and induce the G2/M transition. The scheme incorporates into the model the mode of action of the anticancer drug 5-FU. Cells exposed to 5-FU while in S phase have a higher probability of exiting the cell cycle at the next G2/M transition. The detailed operation of the automaton is schematized step by step in Fig. 10.7 below.

Table 10.1 Parameter values and initial conditions considered in the various figures based on numerical simulations of the cell cycle automaton model. All figures were established for a uniform distribution of durations of cell cycle phases around a mean value, with variability *V*. *Entrainment* The cell cycle is driven by the circadian clock through the circadian variation of Wee1 and Cdk1 (see text for further details). The cell cycle of 22 h duration consists of the following mean durations for the successive phases: G1 (9 h), S (11 h), G2 (1 h), and M (1 h).

Parameter	Conditions			
Cycle length	22 h		22 h	
Circadian entrainment	No entrainment		Entrainment	
Initial conditions	15 000 cells in G1		10 000 cells in steady state[a)]	
Variability (V)	Probability of quitting the cycle (P_0; min^{-1})	Figures	Probability of quitting the cycle (P_0; min^{-1})	Figures
0%	0.0005380	Fig. 10.2a	0.0004925	Figs. 10.2c, 10.6
5%	0.0005380		0.0004930	Fig. 10.6
10%	0.0005380		0.0005000	Fig. 10.6
15%	0.0005380	Fig. 10.2b	0.0005125	Figs. 10.2d, 10.4 10.6
20%	0.0005380		0.0005345	Fig. 10.6

a) Steady-state distribution of phases: 49.1% in G1, 44.2% in S, 3.9% in G2, 2.8% n M.

10.2.2 Distribution of Cell Cycle Phases

The variability in the duration of the cell cycle phases is responsible for progressive cell desynchronization. In the absence of variability, if the duration of each phase is the same for all cells, the population behaves as a single cell. Then, if all cells start at the same point of the cell cycle, e.g. at the beginning of G1, a sequence of square waves bringing the cells synchronously through G1, S, G2, M, and back into G1 occurs (see Fig. 10.2a) (A. Altinok and A. Goldbeter, in preparation). The drop in cell number at the end of the G1 and G2 phases reflects the assumption that exit from the cell cycle occurs at these transitions, to counterbalance the doubling in cell number at the end of M. These square waves continue unabated over time. However, as soon as some degree of variability of the cell cycle phase durations is introduced (Fig. 10.2b), the square waves transform into oscillations through the cell cycle phases, the amplitude of which diminishes as the variability increases. In the long term, these oscillations dampen as the system settles into a steady state distribution of cell cycle phases: the cells are fully desynchronized and have forgotten the initial conditions in which they all started to evolve from the same point of the cell cycle (A. Altinok and A. Goldbeter, in preparation).

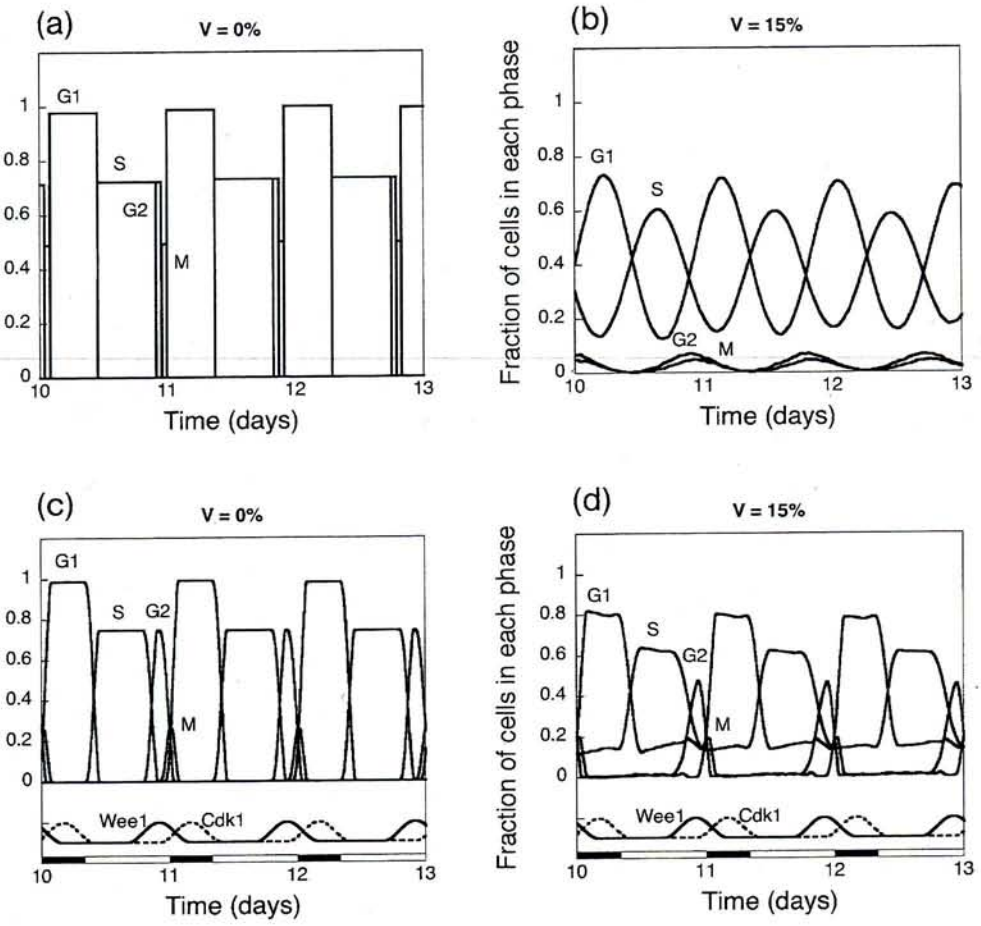

Fig. 10.2 Waves through cell cycle phases in absence (a, b) or presence (c, d) of entrainment by the circadian clock. The variability of durations for all cell cycle phases is equal to 0% (left column) or 15% (right column). The curves, generated by numerical simulations of the cell cycle automaton model, show the proportions of cells in G1, S, G2 or M phase as a function of time, for days 10–13. The time step used for simulations is equal to 1 min. The duration of the cell cycle before or in the absence of entrainment is 22 h. The successive phases of the cell cycle have the following mean durations: G1 (9 h), S (11 h), G2 (1 h), and M (1 h). As explained in the text and in Fig. 10.3a, entrainment by the circadian clock occurs in the model via a semi-sinusoidal rise in Wee1 (from 4 p.m. to 4 a.m.) and a similar, subsequent rise in Cdk1 (from 10 p.m. to 10 a.m.). The variations in Wee1 and Cdk1 from 0 acu to 100 acu (arbitrary concentration units) are represented schematically in panels (c) and (d) below the curves showing the fractions of cells in the various phases. The probability of premature G2/M transition in G2 depends on Cdk1 according to Eq. (2) where $k_C = 0.001$ acu^{-1} (in the simulations we consider that the probability goes to unity if k_C [Cdk1] $\geqslant 1$). The probability of the G2/M transition at the end of G2 depends on Wee1 according to Eq. (1) where $k_W = 0.015$ acu^{-1} (in the simulations we consider that the probability goes to zero when $(1 - k_W$ [Wee1]$) \leqslant 0$). The 24-h light/dark (L/D) cycle is shown as an alternation between an 8-h dark phase (black bar) and a 16-h light phase (white bar). Initial conditions are specified in Table 10.1. The probability of quitting the cycle (in units of 10^{-3} min^{-1}) is equal to 0.5380 for (a) and (c), 0.4925 for (b), and 0.5125 for (d); these values ensure homeostasis of the cell population, i.e. the number of cells in the population oscillates around and eventually reaches a stable steady state value. Panels (a) and (b) start initially with 15 000 cells in G1. Panel (c) and (d) start initially with 10 000 cells in steady state. The data in panels (a) and (b) are normalized by 15 000 cells, in panel (c) by 16 000 and in panel (d) by 14 000 (maximal cell number).

The top panels in Fig. 10.2 show the oscillations in the fraction of cells in the different cell cycle phases, as a function of time, in the absence of entrainment by the circadian clock. In the case considered, the duration of the cell cycle is 22 h, and the variability V is equal to 0% (Fig. 10.2a) or 15% (Fig. 10.2b). When variability is set to zero, no desynchronization occurs and the oscillations in the successive phases of the cell cycle are manifested as square waves that keep a constant amplitude in a given phase. Conversely, when variability increases up to 15% in the absence of entrainment (Fig. 10.2b), the amplitude of the oscillations decreases, reflecting enhanced desynchronization.

10.2.3
Coupling the Cell Cycle Automaton to the Circadian Clock

To determine the effect of circadian rhythms on anticancer drug administration, it is important to incorporate the link between the circadian clock and the cell cycle. Entrainment by the circadian clock can be included in the automaton model by considering that the protein Wee1 undergoes circadian variation, because the circadian clock proteins CLOCK and BMAL1 induce the expression of the *Wee1* gene (see Fig. 10.1b) [3–5]. Wee1 is a kinase that phosphorylates and thereby inactivates the protein kinase cdc2 (also known as the cyclin-dependent kinase Cdk1) that controls the transition G2/M and, consequently, the onset of mitosis.

In mice subjected to a 12:12 light–dark cycle (12 h of light followed by 12 h of darkness), the Wee1 protein level rises during the second part of the dark phase, i.e. at the end of the activity phase. Humans generally keep a pattern in which 16 h of diurnal activity are followed by 8 h of nocturnal sleep. Therefore, when modeling the link between the cell cycle and the circadian clock in humans, we consider a 16:8 light-dark cycle (16 h of light, from 8 a.m. to 12 p.m., followed by 8 h of darkness, from 12 p.m. to 8 a.m.; Fig. 10.3a) [7, 8, 12, 13]. To keep the pattern corresponding to the situation in mice (with a 12-h shift due to the change from nocturnal to diurnal activity) and in agreement with observations in human cells [8], the rise in Wee1 should occur at the end of the activity phase, i.e. with a peak at 10 p.m. The decline in Wee1 activity is followed by a rise in the activity of the kinase Cdk1, which enhances the probability of transition to the M phase. We thus consider that the rise in Wee1 is immediately followed by a similar rise in Cdk1 kinase (see Fig. 10.3a).

In the cell cycle model, we consider that the probability (P) of transition from G2 to M, at the end of G2, decreases as Wee1 rises, according to Eq. (1). Conversely, we assume that the probability of premature transition from G2 to M (i.e. before the end of G2, the duration of which was set when the automaton entered G2) increases with the activity of Cdk1 according to Eq. (2). The probability is first determined with respect to Cdk1; if the G2/M transition has not occurred, the cell progresses in G2. Only at the end of G2 is the probability of transition to M determined as a function of Wee1.

$$P(\text{transition G2} \rightarrow \text{M}) = 1 - k_{\text{w}}[\text{Wee1}] \tag{1}$$

$$P(\text{transition G2} \rightarrow \text{M}) = k_{\text{c}}[\text{Cdk1}] \tag{2}$$

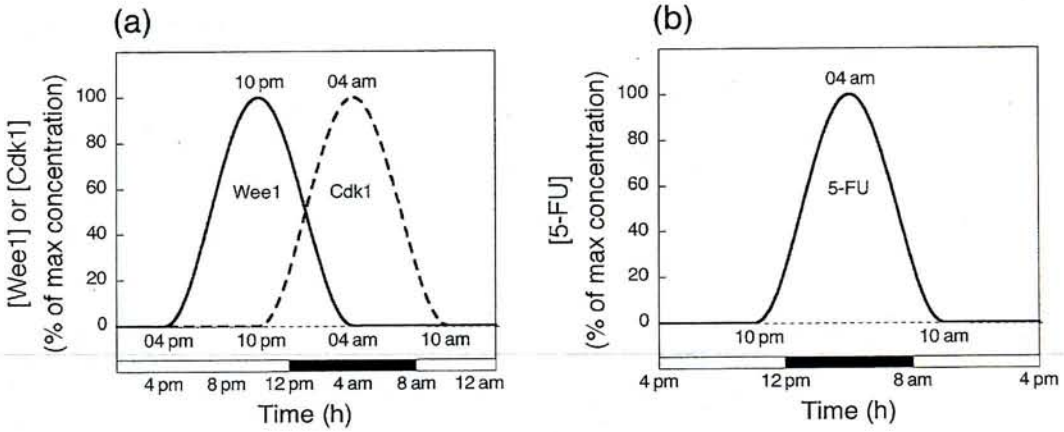

Fig. 10.3 (a) Semi-sinusoidal profile of Wee1 and Cdk1 used for entrainment of the cell cycle by the circadian clock (see text). (b) Semi-sinusoidal administration profile used clinically for 5-FU with peak time at 4 a.m. [30, 31]. Over the 24-h period, the 5-FU level is nil between 10 a.m. and 10 p.m., and rises in a sinusoidal manner between 10 p.m. and 10 a.m. according to Eq. (3), with $A = 100$ and $d = 12$ h, with a peak at 4 a.m. In the model, the probability P of quitting the proliferative compartment at the next G2/M transition after exposure to the drug during the S phase is proportional to [5-FU], according to Eq. (4). At the maximum of [5-FU] reached at 4 a.m., the basal value of the exit probability is multiplied by a factor of 20.

In a previous study [33] we described the rise in Wee1 and Cdk1 by a step increase lasting 4 h. Here, instead of such a square-wave pattern, we will use a temporal pattern of semi-sinusoidal shape. Thus, we assume that Wee1 increases in a semi-sinusoidal manner between 4 p.m. and 4 a.m., with a peak at 10 p.m., while Cdk1 increases in the same manner between 10 p.m. and 10 a.m., with a peak at 4 a.m. (Fig. 10.3a).

Upon entrainment by the circadian clock, cells become more synchronized than in the absence of entrainment. In the case considered in Fig. 10.2c, d, the period changes from 22 h to 24 h, which corresponds to the period of the external LD cycle. When the variability is nil, we observe that the fraction of cells in S phase goes to zero at the trough of the oscillations (Fig. 10.2c). This does not occur when the variability is higher, e.g. 15% (Fig. 10.2d). The fraction of the S-phase cells then oscillates with reduced amplitude, reflecting again the effect of cell cycle desynchronization. However, in contrast to the progressive dampening of the oscillations in the absence of entrainment (Fig. 10.2b), when the cell cycle automaton is driven by the circadian clock oscillations appear to be sustained (Fig. 10.2d).

10.2.4
The Cell Cycle Automaton Model: Relation with Other Types of Cellular Automata

The automaton model for the cell cycle represents a cellular automaton. Because the latter term has been used in a partly different context, it is useful to distinguish the present model from those considered in previous studies. "Cellular automata" are often used to describe the spatiotemporal evolution of chemical or biological

systems that are capable of switching sequentially between several discrete states [34–36]. One typical application of cellular automata pertains to excitable systems (e.g. neurons or muscle cells), which can evolve from a rest state to an excited state, then to a refractory state, before returning to the rest state. Spatially coupled automata can account for the propagation of waves in excitable media. Here, as in the model for the hair follicular cycles [26, 27], we consider spatially independent automata. Thus we assume that, within a population, the dynamics of a cycling cell will not be influenced by the state of neighboring cells. In contrast, in excitable systems, a cell in the rest state can be triggered to switch to the excited state when a neighboring cell is excited. The goal of the present study is to propose an automaton model for the cell cycle, to couple it to the circadian clock, and to use this model to determine the effect of anticancer drugs that kill cells at specific phases of the cell cycle.

10.3
Assessing the Efficacy of Circadian Delivery of the Anticancer Drug 5-FU

10.3.1
Mode of Action of 5-FU

Cells exposed in S phase to 5-FU arrest in this phase as a result of thymidilate synthase inhibition; then, they progress through the cell cycle or die through p53-dependent or independent apoptosis [11]. In the model we consider that cells exposed to 5-FU while in the S phase have an enhanced probability of quitting the proliferative compartment at the next G2/M transition (Fig. 10.1b). The probability of quitting the cycle is taken as proportional to the 5-FU concentration (see Section 10.3.2). We assume that the exit probability in the absence of 5-FU is multiplied by a factor of 20 when the level of 5-FU reaches 100% of its maximum value. Other hypotheses might be retained for the dose–response curve of the drug. Thus, larger or smaller slopes respectively correspond to stronger or weaker cytotoxic effects of 5-FU. A threshold dependence may also be introduced, in which case the linear relationship must be replaced by a sigmoidal curve which tends to a step function as the steepness of the threshold increases.

10.3.2
Circadian Versus Continuous Administration of 5-FU

In simulating the cell cycle automaton response to 5-FU, we impose a circadian profile of the anticancer medication similar to that used in clinical oncology [30, 31]: 5-FU is delivered in a semi-sinusoidal manner from 10 p.m. to 10 a.m., with a peak at 4 a.m. (Fig. 10.3b). During the remaining hours of the day and night, the drug concentration is set to zero. For comparison, we consider similar drug delivery patterns shifted in time, with peak delivery either at 10 a.m., 4 p.m., or 10 p.m.

The semi-sinusoidal delivery of the anticancer drug obeys the following equation which yields the concentration, [5-FU], as a function of time over the 24-h period:

$$[\text{5-FU}] = (A/2)[1 - \cos(2\pi(t - t_{\text{start}})/d)] \tag{3}$$

For delivery over a period d starting at 10 p.m. and ending at 10 a.m. and with a peak at 4 a.m., we take $t_{\text{start}} = 22$ h and $d = 12$ h, with $A = 100$. The probability (P) of exiting the cell cycle after exposure to a given level of 5-FU during the S phase is given by Eq. (4):

$$P = P_0(1 + k_f[\text{5-FU}]) \tag{4}$$

The value of P_0 is chosen so as to ensure tissue homeostasis, i.e. near constancy of the total cell number when cell proliferation is roughly compensated by cell death in the absence of anticancer drug treatment (such an assumption might not hold for tumoral tissues, in which case P_0 should be smaller than the value corresponding to homeostasis). The concentration of 5-FU, denoted [5-FU], varies from 0 to 100 (arbitrary units). Parameter k_f measures the cytotoxicity of 5-FU: the larger k_f, the larger the probability of quitting the cell cycle after exposure to the drug during the S phase. The values of P_0 used in numerical simulations are listed in Table 10.1. We choose the value $k_f = 0.19$ so that the probability of quitting the cell cycle is multiplied by 20 at the maximum 5-FU concentration.

It is useful to compare the circadian patterns of 5-FU delivery with the more conventional constant infusion drug-delivery pattern, in which the amount of 5-FU delivered over the 24-h period is the same as for the circadian delivery schedules. The quantity of 5-FU (Q_{5FU}) delivered over 24 h according to the semi-sinusoidal schedule defined by Eq. (3) is given by Eq. (5):

$$Q_{5\text{FU}} = \int_0^d \frac{A}{2}\left(1 - \cos\left(\frac{2\pi t}{d}\right)\right) dt = \frac{A}{2}(d + \sin 2\pi - \sin 0) = \frac{A}{2}d \tag{5}$$

For $A = 100$ [in arbitrary concentration units (acu)] and $d = 12$ h, this expression yields a mean 5-FU level of 25 acu, which is used for the case of constant infusion in Figs. 10.4b and 10.5e.

10.3.3
Circadian 5-FU Administration: Effect of Time of Peak Drug Delivery

The cytotoxic effect of the circadian administration of 5-FU depends on a variety of factors, which we consider in turn below. These factors include the mean duration D of the cell cycle phases, the variability V of cell cycle phase durations, entrainment by the circadian clock, and timing of the daily peak in 5-FU. For definiteness we consider the case where the cell cycle length, in the absence of entrainment, is equal to 22 h.

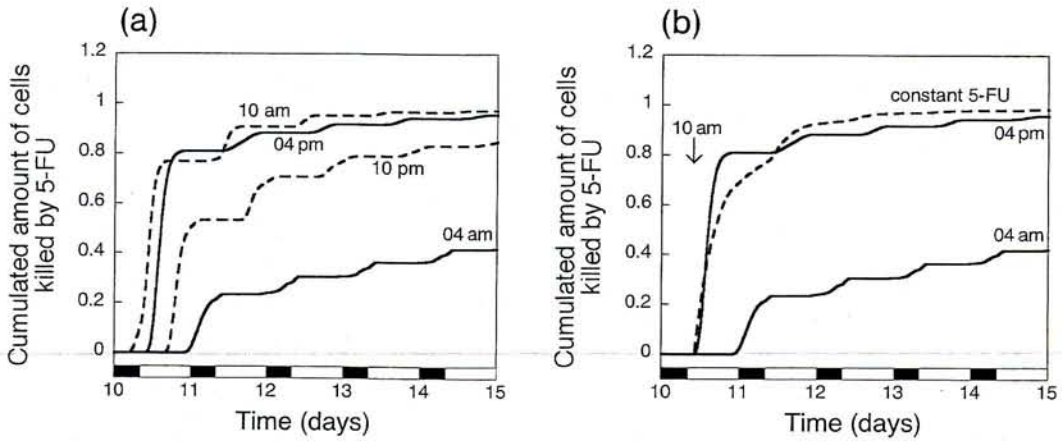

Fig. 10.4 (a) Cytotoxicity of chronomodulated 5-FU: effect of various circadian schedules of 5-FU delivery peaking at various times (4 a.m., 10 a.m., 4 p.m., 10 p.m.), when variability V is equal to 15%. (b) The circadian patterns peaking at 4 a.m. or 4 p.m. are compared with continuous delivery of 5-FU, which begins at 10 a.m. on day 10 (vertical arrow). The curves in (a) and (b) show the cumulated cell kill for days 10–15, in the presence of entrainment by the circadian clock. Prior to entrainment the cell cycle duration is 22 h. Parameter values and initial conditions are given in Table 10.1. The data are normalized by the mean cell number, 10 800.

To investigate the effect of the peak time of circadian delivery of 5-FU, we compare in Fig. 10.4a four circadian schedules with peak delivery at 4 a.m., 10 a.m., 4 p.m., and 10 p.m., for a cell cycle variability of 15%. The data on cumulated cell kill by 5-FU indicate a sharp difference between the circadian schedule with a peak at 4 a.m., which is the least toxic, and the other schedules. This difference is even more striking when cells are better synchronized, for smaller values of variability V (data not shown). The most toxic circadian schedules are those with a peak delivery at 4 p.m. or 10 a.m. We compare in Fig. 10.4b the least and most toxic circadian patterns of 5-FU delivery with the continuous infusion of 5-FU. Continuous delivery of 5-FU appears to be slightly more toxic than the circadian pattern with a peak at 4 p.m.

To clarify the reason why different circadian schedules of 5-FU delivery have distinct cytotoxic effects, we used the cell cycle automaton model to determine the time evolution of the fraction of cells in S phase in response to different patterns of circadian drug administration, for a cell cycle variability of 15%. The results, shown in Fig. 10.5, correspond to the case considered in Fig. 10.4, namely, entrainment of a 22-h cell cycle by the circadian clock. The data for Fig. 10.5a clearly indicate why the circadian schedule with a peak at 4 a.m. is the least toxic. The reason is that the fraction of cells in S phase is then precisely in antiphase with the circadian profile of 5-FU. Since 5-FU only affects cells in the S phase, the circadian delivery of the anticancer drug in this case kills but a negligible amount of cells.

When the peak delivery of 5-FU is at 4 p.m., the situation is opposite: now, the phase of 5-FU administration precisely coincides with the time period during which the majority of cells pass through the S phase (Fig. 10.5c). As a result, the first peak in S-phase cells is nearly annihilated following drug exposure. The remaining cells die after exposure to the second 5-FU pulse, which again coincides

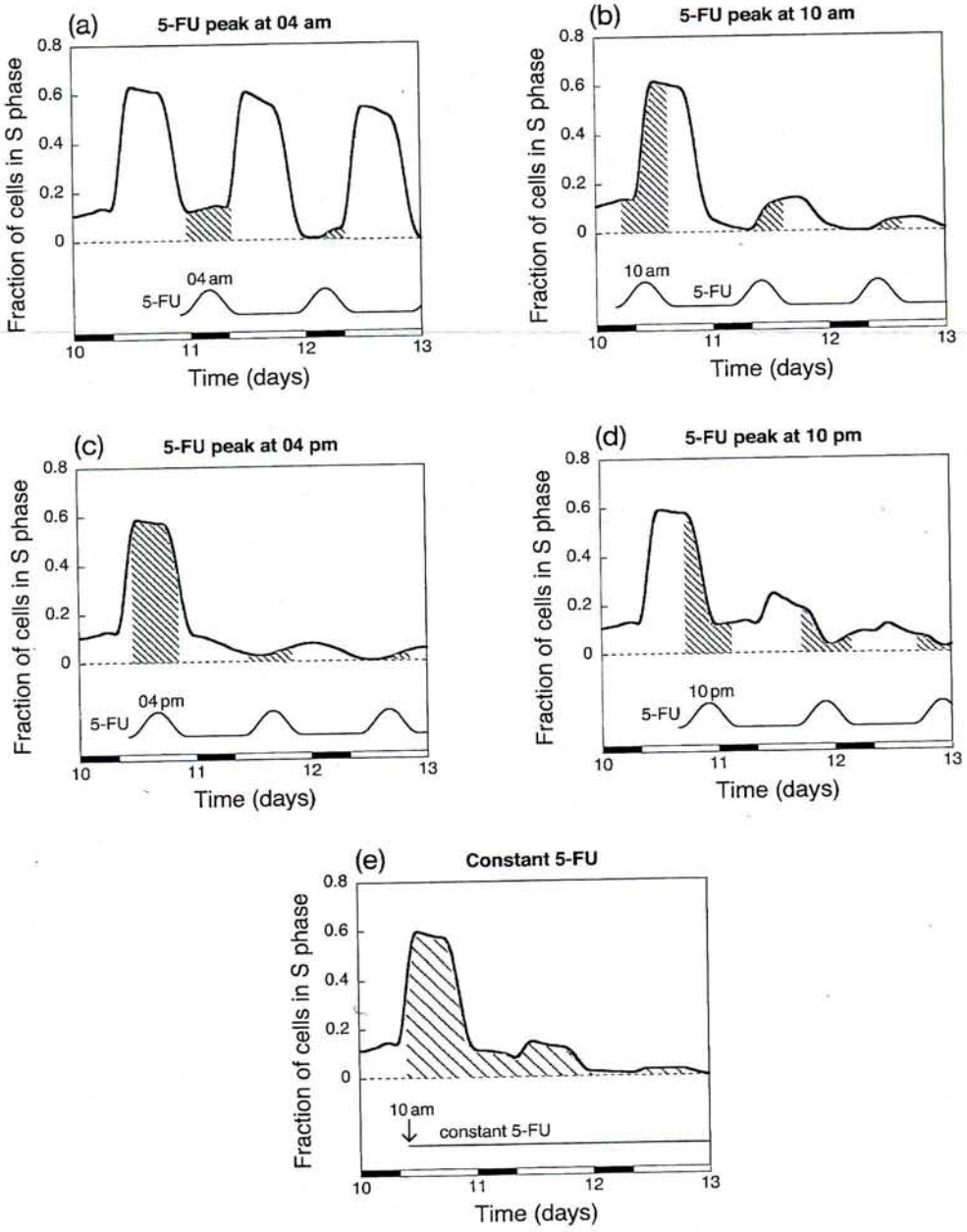

Fig. 10.5 Explanation of the cytotoxic effect of various circadian schedules of 5-FU delivery with peak at 4 a.m. (a), 10 a.m. (b), 4 p.m. (c), or 10 p.m. (d), and of continuous 5-FU delivery (e). Data are obtained for variability $V = 15\%$ and for a cell cycle duration of 22 h, in the presence of entrainment by the circadian clock. The hatched area shows the fraction of cells in S phase exposed to 5-FU and thus likely marked to exit the cell cycle at the next G2/M transition. The curves in Fig. 10.4 showing the cumulated number of cells killed indicate that the schedule with peak delivery at 4 a.m. is the one that causes minimal damage to the cells because the peak in 5-FU then coincides with the trough of the oscillations of S-phase cells. Continuous delivery of 5-FU is nearly as toxic as the most toxic circadian schedule of 5-FU delivery that peaks at 4 p.m. Because 5-FU is delivered at a constant, intermediate value in panel (e), the probability of exiting the cell cycle is enhanced but not as much as at the peak of the semi-sinusoidal delivery illustrated in the other panels. Hatching marks are thus more spaced in panel (e) to indicate this effect. Parameter values and initial conditions are given in Table 10.1. The data are normalized by the maximal cell number, 14 000.

with the next peak of S-phase cells. The latter peak is much smaller than the first one, because most cells exited the cycle after exposure to the first 5-FU pulse.

The cases of peak delivery at 10 a.m. (Fig. 10.5b) or 10 p.m. (Fig. 10.5d) are intermediate between the two preceding cases. Overlap between the peak of 5-FU and the peak of cells in S phase is only partial, but it is still greater in the case of the peak at 10 a.m., so that this pattern is the second most toxic, followed by the circadian delivery centered around 10 p.m. The comparison of the four panels Fig. 10.5a–d explains the results of Fig. 10.4a on the marked differences in cytotoxic effects of the four 5-FU circadian delivery schedules. The use of the cell cycle automaton helps clarify the dynamic bases that underlie the distinctive effects of the peak time in the circadian pattern of anticancer drug delivery.

The comparison between the curves in Figs. 10.4a and 10.5b and c raises the question of why the cytotoxic effect of 5-FU is nearly similar for the patterns in which 5-FU peaks at 4 p.m. and 10 a.m. (Fig. 10.4a), despite the fact that the peak in S phase cells presents a better overlap with the peak in 5-FU (the overlap is indicated by the dashed area under the fraction of S phase cells) when 5-FU peaks at 4 p.m. (Fig. 10.5c) compared with 10 a.m. (Fig. 10.5b). The reason is saturation in the cytotoxic effect of 5-FU. When the cytotoxic effect of 5-FU measured by parameter k_f is sufficiently large, most cells exposed to 5-FU during the first part of the S-phase peak in the case of Fig. 10.5c are already marked for exiting the cell cycle at the next G2/M transition, so that few additional cells are killed by 5-FU during the second part of the S-phase peak even though it corresponds to the 5-FU peak. Nearly the same amount of cells are marked for exiting the cycle after exposure to 5-FU during the first part of the S-phase peak in the case of Fig. 10.5b, because this fraction of the S-phase peak corresponds to the peak of 5-FU. To test this explanation we reduced the value of parameter k_f from 0.19 to 0.04, so that the maximum probability of quitting the cycle following exposure to 5-FU passes from $20P_0$ to $5P_0$ when 5-FU reaches its maximum value of 100 (see Eq. 4). As predicted, we observe a somewhat stronger differential effect between the patterns of 5-FU peaking at 4 p.m. and 10 a.m. when the value of k_f is reduced (data not shown).

When cells are more synchronized, e.g. in the presence of entrainment by the circadian clock for a variability of 5%, the results are similar, but the cytotoxic effect of the drug is decreased or enhanced depending on whether the peak of 5-FU occurs at 4 a.m. or 4 p.m., respectively (data not shown). Thus, for a peak delivery of 5-FU at 4 a.m., drug delivery is still in antiphase with the oscillation in S-phase cells, but because cells are more synchronized the fraction of S cells goes to zero at its trough. As a result, very few cells remain in S phase during the 5-FU pulse, so that only a minute cytotoxic effect is observed. For the pattern with peak drug delivery at 4 p.m., the situation is again close to the case of Fig. 10.5c: the peak of 5-FU precisely overlaps with the peak of cells in S phase, but because cells are more synchronized the amplitude of the peak in S cells is larger. The amount of cells killed after the first 5-FU pulse is thus larger than in the case when cells are less synchronized. Here again most cells killed by 5-FU exit the cycle after the first pulse of the drug.

The case of the continuous infusion of 5-FU is considered in Fig. 10.5e. Because the total amount of 5-FU administered over 24 h is the same as for the circadian semi-sinusoidal patterns, the level of 5-FU – and hence the cytotoxic effect of the drug – is sometimes below and sometimes above that reached with the circadian schedule. The numerical simulations of the automaton model indicate that the cytoxicity is comparable to that observed for the most toxic circadian pattern, with peak delivery of 5-FU at 4 p.m.

A systematic investigation of the effect of the timing of the 5-FU peak on cell cytotoxicity indicates that the cytotoxic effect reaches its trough when the peak time of 5-FU is around 3 a.m., then rises progressively when the peak time increases up to 8 a.m. before reaching a plateau for peak times between 9 a.m. and 9 p.m., and finally drops when the peak time goes from 10 p.m. to 3 a.m. These results corroborate, with a higher degree of resolution, those illustrated in Figs. 10.4 and 10.5.

All the above results have been obtained for the case where the durations of the various cell cycle phases obey a probability distribution centered around the mean duration D, with a range of variation extending uniformly from $D - V$ to $D + V$. Similar results are obtained when assuming that the probability distribution obeys a lognormal distribution centered around the same mean value [33].

10.3.4
Effect of Variability of Cell Cycle Phase Durations

We have already alluded to the effect of synchronization governed by variability V. To further address this point, Fig. 10.6 shows, as a function of V, the cytotoxic effect of the 5-FU profile considered in Fig. 10.2b, with the peak at 4 a.m., in the presence of entrainment of the 22-h cycle by the circadian clock. The results indicate that the cumulated cell kill increases when V rises from 0% to 20%. For this circadian schedule of 5-FU, which is the least toxic to the cells (see above), we see that the better the synchronization, the smaller the number of cells killed. Here, in the presence of entrainment, a larger increase occurs between $V \leqslant 10\%$ and $V \geqslant 15\%$ in the number of cells killed by the drug. This jump is not observed in the absence of entrainment (data not shown). Entrainment by the circadian clock further enhances the synchronization of cells and protects them from the drug, as long as V remains relatively small, i.e. $V \leqslant 10\%$. Therefore, circadian entrainment magnifies the consequences of cell cycle variability, as it introduces a threshold in the effect of this parameter.

The effect of variability on drug cytotoxicity markedly depends on the temporal pattern of 5-FU delivery. When the peak in the circadian delivery of 5-FU occurs at 4 p.m., i.e. when the circadian schedule of 5-FU administration is most toxic to the cells, whether in the absence or presence of entrainment by the circadian clock, cytotoxicity increases as the degree of variability decreases. The effect is more marked in the conditions of entrainment: a threshold in cytotoxicity then exists between $V = 10\%$ and 15% (data not shown). Thus, in contrast to what is observed for the pattern of 5-FU peaking at 4 a.m. (Fig. 10.6), for the circadian 5-FU delivery sched-

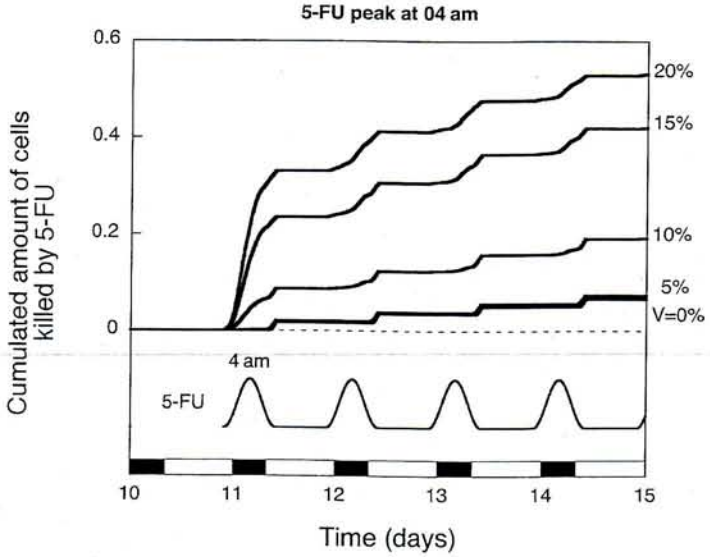

Fig. 10.6 Cytotoxicity of chronomodulated 5-FU: effect of variability of cell cycle phase durations. Shown is the cumulative cell kill when 5-FU is delivered in a circadian manner with peak at 4 a.m., in the presence of entrainment by the circadian clock, for different values of variability V indicated on the curves. The cell cycle duration is 22 h. Initial conditions and probabilities of exiting the cell cycle are specified in Table 10.1. Cell kill is normalized by the mean cell number, i.e. 13 000 for $V = 0\%$ and $V = 5\%$, 11 400 for $V = 10\%$, 10 800 for $V = 15\%$, and 10 700 for $V = 20\%$.

ule that peaks at 4 p.m, enhanced synchronization through decreased variability does not protect cells, but rather it increases their sensitivity to 5-FU cytotoxicity. This leads us to conclude that variability has opposite effects on cytotoxicity when the circadian delivery pattern of 5-FU peaks at 4 p.m. versus 4 a.m.

Numerical simulations therefore indicate that the least damage to the cells occurs when the peak of 5-FU circadian delivery is at 4 a.m., and when cells are well synchronized, i.e., when cell cycle variability V is lowest. In contrast, when the peak of 5-FU circadian delivery is at 4 p.m., cytotoxicity is enhanced when cells are well synchronized. The cytotoxic effect of the drug, therefore, can be enhanced or diminished by increased cell cycle synchronization, depending on the relative phases of the circadian schedule of drug delivery and the cell cycle entrained by the circadian clock. Continuous infusion of 5-FU is nearly as toxic as the most cytotoxic circadian pattern of anticancer drug delivery.

10.4 Discussion

The study of various anticancer drugs shows that many possess an optimal circadian delivery pattern, according to the phase of the cell cycle in which the cytotoxic effect is exerted. A case in point is provided by 5-FU. This widely used anticancer drug interferes with DNA synthesis and acts during DNA replication, the S phase of the cell cycle. Cells exposed to 5-FU during the S phase have an enhanced proba-

bility of dying from apoptosis at the next G2/M transition. In humans, the circadian pattern of 5-FU administration with peak delivery at 4 a.m. is the least cytotoxic; and the pattern with peak delivery at 4 p.m. is the most cytotoxic. In addition, for reasons which are still unclear, maximum 5-FU cytotoxicity to tumor cells occurs at the same time as best 5-FU tolerance, i.e. minimal damage to healthy tissues. In anticancer treatment, 5-FU is therefore administered according to a semi-sinusoidal pattern with peak delivery at 4 a.m. [30, 31].

It would be useful to base these empirical results on the effect exerted by the anticancer drug on the cell cycle in tumor and normal cells. This would not only help explain the dependence of cytotoxicity and tolerance on the temporal pattern of drug administration, but it would also provide firm foundations at the cellular level for the chronotherapeutical approach. To investigate the link between the cell cycle and the circadian clock and to assess the effect of circadian patterns of anticancer drug delivery, it is useful to resort to a modeling approach. Computational models allow a rapid exploration of a molecular or cellular mechanism over a wide range of conditions [16, 17, 33]. To assess the effect of various temporal patterns of anticancer drug administration we need a model for the cell cycle, allowing the study of its coupling to the circadian clock and of the effect of cytotoxic drugs. Rather than resorting to a detailed molecular model for the cell cycle in terms of cyclins and cyclin-dependent kinases and their control – models of this sort are available [17–22] and are currently being extended (C. Gérard and A. Goldbeter, in preparation) – we used here a phenomenological approach in which the progression between the successive phases of the cell cycle is described by a stochastic automaton.

The cell cycle automaton switches sequentially between the phases G1, S, G2, and M, with a probability P related to the duration of the various cell cycle phases. Each phase is characterized by its mean duration D and by its variability V. Upon mitosis (phase M), cells divide and enter a new cycle in G1. Exit from the cell cycle, reflecting cell death, occurs at the G1/S and G2/M transitions. Appropriate values of the exit probability allow for homeostasis of the total cell population. The anticancer drug 5-FU augments the exit probability for those cells that have been exposed to 5-FU during the S phase of DNA replication. An advantage of the stochastic automaton model is that it can readily be simulated to probe the cytotoxic effect of various circadian or continuous patterns of anticancer drug delivery. We showed that the cell cycle automaton model can be entrained by the circadian clock when incorporating a circadian block of the transition between the G2 and M phases, reflecting the circadian increase in the kinase Wee1. This increase takes place at the time set by the rise of the circadian clock protein BMAL1 in humans. Likewise, we incorporated the effect of the circadian increase in the kinase Cdk1, which immediately follows the peak in Wee1. The effect of Cdk1 corresponds in the model to an enhanced probability of transition between the G2 and M phases. The detailed operation of the cell cycle automaton model for a given cell i from G1 to mitosis is schematized step by step in Fig. 10.7.

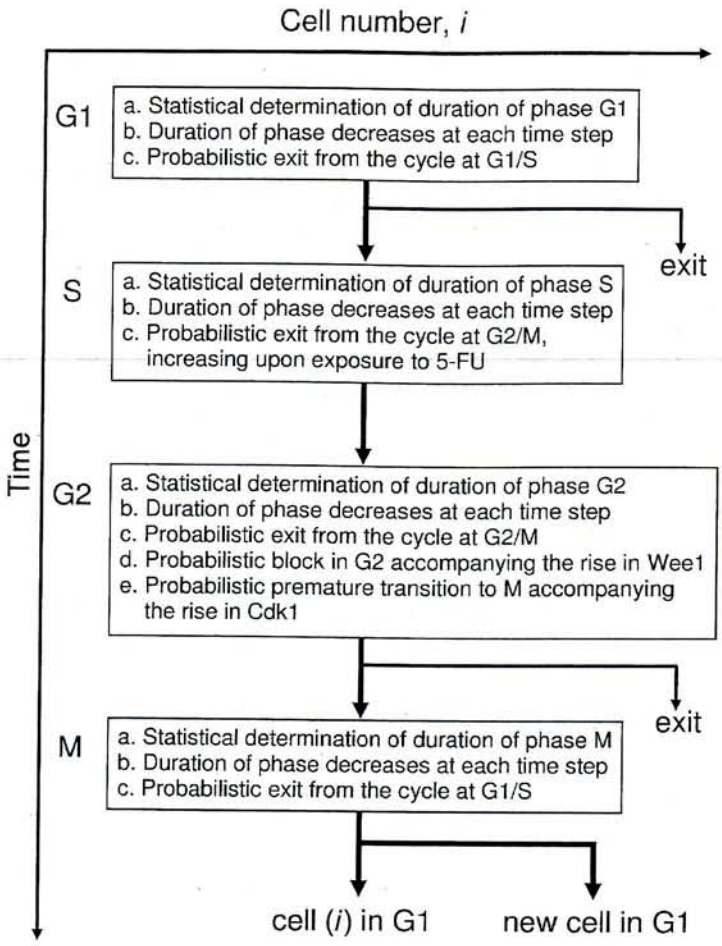

Fig. 10.7 Scheme of the operation of the cell cycle automaton step by step, from G1 to M phase.

Coupling the cell cycle automaton to the circadian variation of Wee1 and Cdk1 permits entrainment of the cell cycle by the circadian clock, at a phase that is set by the timing of the peak of the circadian clock protein BMAL1. Entrainment strengthens cell synchronization. The peak of cells in S phase is of particular relevance for the action of 5-FU. The model predicts, upon entrainment by the circadian clock, that in humans the fraction of cells in S phase reaches a maximum during the light phase, around 4 p.m., while it reaches its minimum during night, around 4 a.m. (Fig. 10.2c, d).

We compared the effect of the continuous administration of 5-FU with various circadian patterns of 5-FU delivery peaking at 4 a.m, 10 a.m., 4 p.m., or 10 p.m. in the presence of entrainment by the circadian clock, by measuring the normalized, cumulative number of cells killed by 5-FU (Fig. 10.4). Several conclusions can be drawn from this comparison. First, the various circadian patterns of 5-FU delivery have markedly different cytotoxic effects on diurnally active cancer patients: the least toxic pattern is that which peaks at 4 a.m., while the most toxic one is that which peaks at 4 p.m. The other two patterns peaking at 10 a.m. or 10 p.m. exert intermediate cytotoxic effects. Conventional continuous infusion of 5-FU is nearly as toxic as the circadian pattern of 5-FU delivery peaking at 4 p.m.

The cell cycle automaton model permits us to clarify the reason why circadian delivery of 5-FU is least or most toxic when it peaks at 4 a.m. or 4 p.m., respectively. Indeed, the model allows us to determine the position of the peak in S-phase cells relative to that of the peak in 5-FU. As shown in Fig. 10.5, 5-FU is least cytotoxic when the fraction of S-phase cells oscillates in antiphase with 5-FU (when 5-FU peaks at 4 a.m.) and most toxic when both oscillate in phase (when 5-FU peaks at 4 p.m). Intermediate cytotoxicity is observed for other circadian patterns of 5-FU (when the drug peaks at 10 a.m. or 10 p.m.), for which the peak of 5-FU partially overlaps with the peak of S-phase cells. For the continuous infusion of 5-FU, the peak in S-phase cells necessarily occurs in the presence of a constant amount of 5-FU. Hence, the constant delivery pattern is nearly as toxic as the circadian pattern peaking at 4 p.m.

The goal of anticancer chronotherapies is to maximize the cytotoxic effect of medications on the tumor while protecting healthy tissues. The question arises as to how the above results might be used to predict the differential effect of an anticancer drug such as 5-FU on normal and tumor cell populations. This issue relates to the ways in which normal and tumor cells differ [13]. Such differences may pertain to the characteristics of the cell cycle, e.g. duration of the cell cycle phases and their variability, or entrainment of the cell cycle by the circadian clock. Such differences have been encountered in experimental tumor models [37, 38]. Thus both the molecular circadian clock and the 24-h pattern in cell cycle phase distribution depended upon the growth stage of Glasgow osteosarcoma in mice. In this rapidly growing tumor with a doubling time of $\sim$ 2 days, both circadian and cell cycle clocks were present yet altered at an early stage and became ablated when the tumor grew bigger [39]. The clinical relevance of these findings is supported by heterogeneous and usually decreased expression of clock genes in human tumors [40–43].

The results of simulations indicate that, when the circadian delivery of 5-FU peaks at 4 a.m., differential effects of the drug on a population of healthy cells and on a population of tumor cells may be observed depending on whether the two cell populations are entrained or not by the circadian clock [33]. Another source of differential effect pertains to the degree of variability, given that, as previously noted, synchronization of the cells minimizes cytotoxic damage when the circadian 5-FU modulated delivery pattern peaks at 4 a.m. The results are markedly different when the circadian pattern of 5-FU delivery peaks at 4 p.m. [33]. Then the cytotoxic effect of the drug on the two populations is the inverse as that predicted for the circadian pattern peaking at 4 a.m. The effect of variability therefore depends on the circadian pattern of 5-FU delivery and on the possibility of entrainment of the cell cycle by the circadian clock.

The results presented here point to the interest of measuring, both in normal and tumor cell populations, parameters such as the duration of the cell cycle phases and their variability, as well as the presence or absence of entrainment by the circadian clock. As shown by the results obtained with the cell cycle automaton model, these data are crucial for using the model to predict the differential outcome of various anticancer drug delivery schedules on normal and tumor cell populations. In a sub-

sequent step, we plan to incorporate pharmacokinetic–pharmacodynamic (PK-PD) aspects of 5-FU metabolism into the modeling approach. Thus, the enzymatic activities responsible for the catabolism of 5-FU and the generation of its cytotoxic forms display opposite circadian patterns in healthy tissues [29].

The results presented here show that the cell cycle automaton model displays a high sensitivity to the rate of spontaneous exit from the cell cycle. Progressive explosion or extinction of the cell population occurs for a value of the exit rate slightly above or below the value yielding homeostasis, i.e. stabilization of the cell count which oscillates in a constant range without displaying any oscillatory exponential increase or decrease. This result stresses the physiological importance of this parameter, which is likely controlled by the cell population as a function of total cell mass. Homeostasis may easily be guaranteed when such auto-regulation is implemented in the model by making the exit probability P_0 depend on the total cell number N, e.g. by replacing P_0 by the expression $P = P_0 + R[(N/N_s) - 1]$, where R is a parameter measuring the strength of regulation, and N_s denotes the number of cells in the population above or below which P_0 is respectively increased or decreased.

The present modeling approach to circadian cancer chronotherapy is based on an automaton model for the cell cycle. Continuous approaches to cell cycle progression have also been used to study the link between cell proliferation and circadian rhythms [44] and to determine, in conjunction with optimal control theory, the most efficient circadian schedules of anticancer drug administration [45]. Including more molecular details of the cell cycle in continuous models for cell populations represents a promising line for future research. Hybrid models incorporating molecular details into the automaton approach presented here will also likely be developed.

Besides circadian cancer chronotherapy, another line of research resorting to periodic schedules of anticancer drug delivery has been proposed and analyzed theoretically [46–49]. It is based on a resonance phenomenon between the period of drug administration and the cell cycle time of normal tissue. The goal of this approach is again to develop a strategy that limits, as much as possible, damage to normal sensitive tissue, while maximizing the destruction of tumor cells. While the assessment of circadian cancer chronotherapy has for long been the topic of multicenter clinical studies, the approach based on resonance in periodic chemotherapy is supported so far by a limited number of experimental studies in mice [50, 51], but has yet to be tested clinically. The main idea behind the latter approach is that the periodic scheduling of phase-specific cytotoxic agents can increase the selectivity of therapy when the treatment period is close to the mean cycle length of proliferation of normal susceptible cells, provided the cell cycle time of normal cells differs from that of malignant cells. Damage to the population of normal cells should thus remain limited when chemotherapy is administered with a period close to the normal cell cycle time. In contrast, each dose of chemotherapy should kill another fraction of the tumor cell population because the latter cells divide with a different periodicity.

The phenomenon of resonance in periodic chemotherapy has been analyzed further in more refined cell population models [52]. Potential difficulties inherent in this approach were examined by means of a theoretical model of acute myelogenous leukemia [53]. The authors concluded that chronotherapy based on the resonance effect is unlikely to be efficacious in the treatment of this particular disease. One reason is that the treatment itself may alter the kinetic parameters characterizing the tumor in such a way that the average intermitotic interval varies in the course of chemotherapy. The resonance-based efficiency of chronotherapy might wane if the difference of cell cycle length between normal and malignant cells declines as a result of drug administration.

To some extent the idea of resonance is also present in the case of circadian 5-FU delivery. Indeed, the circadian patterns of 5-FU which peak at 4 a.m. or 4 p.m. correspond to oscillations that are, respectively, in antiphase or in corresponding phase with the circadian variation of the fraction of cells in S phase. This effect can be seen even for cell cycle durations that differ from 24 h, because of the entrainment of the cell cycle by the circadian clock.

Here, as in a previous publication [33], we used the cell cycle automaton model to probe the cytotoxic effect of various patterns of circadian or continuous 5-FU delivery. The results provide a framework to account for experimental and clinical observations, and to help us predict optimal modes of drug delivery in cancer chronotherapy. By explaining the differential cytotoxicity of various circadian schedules of 5-FU delivery, the model clarifies the foundations of cancer chronotherapeutics. In view of its versatility and reduced number of parameters, the automaton model could readily be applied to probe the administration schedules of other types of anticancer medications active on other phases of the cell cycle.

Acknowledgments

This work was supported by the *Fonds de la Recherche Scientifique Médicale* (F.R.S.M., Belgium) through grant 3.4636.04 and by the European Union through the Network of Excellence BioSim, Contract No. LSHB-CT-2004-005137. This study was performed while one of the authors (A.G.) held a *Chaire Internationale de Recherche Blaise Pascal de l'Etat et de la Région Ile-de-France, gérée par la Fondation de l'Ecole Normale Supérieure* in the Institute of Genetics and Microbiology at the University of Paris-Sud 11 (Orsay, France).

References

1 Fu, L., Pelicano, H., Liu, J., Huang, P., Lee, C.C.: The circadian gene Period2 plays an important role in tumor suppression and DNA damage response in vivo. *Cell* **2002**, 111:41–50.

2 Filipski, E., King, V.M., Li, X.M., Granda, T.G., Mormont, M.C., Liu, X., Claustrat, B., Hastings, M.H., Levi, F.: Host circadian clock as a control point in tumor progression. *J. Natl Cancer Inst.* **2002**, 94:690–697.

3 Matsuo, T., Yamaguchi, S., Mitsui, S., Emi, A., Shimoda, F., Okamura, H.: Control mechanism of the circadian clock for timing of cell division in vivo. *Science* **2003**, 302:255–259.

4 Hirayama, J., Cardone, L., Doi, M., Sassone-Corsi, P.: Common pathways in circadian and cell cycle clocks: light-dependent activation of Fos/AP-1 in zebrafish controls CRY-1a and WEE-1. *Proc. Natl Acad. Sci. USA* **2005**, 102:10194–10199.

5 Reddy, A.B., Wong, G.K.Y., O'Neill, J., Maywood, E.S., Hastings, M.H.: Circadian clocks: neural and peripheral pacemakers that impact upon the cell division cycle. *Mutat. Res.* **2005**, 574:76–91.

6 Smaaland, R.: Circadian rhythm of cell division. *Prog. Cell Cycle Res.* **1996**, 2:241–266.

7 Bjarnason, G.A., Jordan, R.: Circadian variation of cell proliferation and cell cycle protein expression in man: clinical implications. *Prog. Cell Cycle Res.* **2000**, 4:193–206.

8 Bjarnason, G.A., Jordan, R.C.K., Wood, P.A., Li, Q., Lincoln, D.W., Sothern, R.B., Hrushesky, W.J.M., Ben-David, Y.: Circadian expression of clock genes in human oral mucosa and skin. *Am. J. Pathol.* **2001**, 158:1793–1801.

9 Granda, T.G., Liu, X.H., Smaaland, R., Cermakian, N., Filipski, E., Sassone-Corsi, P., Lévi, F.: Circadian regulation of cell cycle and apoptosis proteins in mouse bone marrow and tumor. *FASEB J.* **2005**, 19:304–306.

10 Focan, C.: Circadian rhythms and cancer chemotherapy. *Pharm. Ther.* **1995**, 67:1–52.

11 Lévi, F.: Chronopharmacology of anticancer agents. In: Redfern, P.H., Lemmer, B. (eds), *Physiology and Pharmacology of Biological Rhythms* (*Handbook of Experimental Pharmacology, Vol. 125*), Springer-Verlag, Berlin, **1997**, pp 299–331.

12 Lévi, F.: Circadian chronotherapy for human cancers. *Lancet Oncol.* **2001**, 2:307–315.

13 Granda, T., Lévi, F.: Tumor based rhythms of anticancer efficacy in experimental models. *Chronobiol. Int.* **2002**, 19:21–41.

14 Lévi F.: From circadian rhythms to cancer chronotherapeutics. *Chronobiol. Int.* **2002**, 19:1–19.

15 Mormont, M.C., Lévi, F.: Cancer chronotherapy: principles, applications, and perspectives. *Cancer* **2003**, 97:155–169.

16 Goldbeter, A., Claude, D.: Time-patterned drug administration: Insights from a modeling approach. *Chronobiol. Int.* **2002**, 19:157–175.

17 Goldbeter, A.: *Biochemical Oscillations and Cellular Rhythms*, Cambridge University Press, Cambridge, **1996**.

18 Tyson, J.J., Novak, B.: Regulation of the eukaryotic cell cycle: molecular antagonism, hysteresis, and irreversible transitions. *J. Theor. Biol.* **2001**, 210:249–263.

19 Swat, M., Kel, A., Herzel, H.: Bifurcation analysis of the regulatory modules of the mammalian G1/S transition. *Bioinformatics* **2004**, 20:1506–1511.

20 Qu, Z., MacLellan, W.R., Weiss, J.N.: Dynamics of the cell cycle: checkpoints, sizers, and timers. *Biophys. J.* **2003**, 88:3600–3611.

21 Chassagnole, C., Jackson, R.C., Hussain, N., Bashir, L., Derow, C., Savin, J., Fell, D.A.: Using a mammalian cell cycle simulation to interpret differential kinase inhibition in anti-tumour pharmaceutical development. *BioSystems* **2006**, 83:91–97.

22 Csikasz-Nagy, A., Battogtokh, D., Chen, K.C., Novak, B., Tyson, J.J.: Analysis of a generic model of eukaryotic cell-cycle regulation. *Biophys J.* **2006**, 90:4361–4379.

23 Smith, J.A., Martin, L.: Do cells cycle? *Proc. Natl Acad. Sci. USA* **1973**, 70:1263–1267.

24 Brooks, R.F., Bennett, D.C., Smith, J.A.: Mammalian cell cycles need two random transitions. *Cell* **1980**, 19:493–504.

25 Cain, S.J., Chau, P.C.: Transition probability cell cycle model. I. Balanced growth. *J. Theor. Biol.* **1997**, 185:55–67.

26 Halloy, J., Bernard, B.A., Loussouarn, G., Goldbeter, A.: Modeling the dynamics of human hair cycles by a follicular automaton. *Proc. Natl Acad. Sci. USA* **2000**, 97:8328–8333.

27 Halloy, J., Bernard, B.A., Loussouarn, G., Goldbeter, A.: The follicular automaton model: effect of stochasticity and of synchronization of hair cycles. *J. Theor. Biol.* **2002**, 214:469–479.

28 Metzger, G., Massari, C., Etienne, M.C., Comisso, M., Brienza, S., Touitou, Y., Milano, G., Bastian, G., Misset, J.L., Levi, F.: Spontaneous or imposed circadian changes in plasma concentrations of 5-fluorouracil coadministered with folinic acid and oxaliplatin: relationship with mucosal toxicity in patients with cancer. *Clin. Pharmacol. Ther.* **1994**, 56:190–201.

29 Zhang, R., Lu, Z., Liu, T., Soong, S.J., Diasio, R.B.: Relationship between circadian-dependent toxicity of 5-fluorodeoxyuridine and circadian rhythms of pyrimidine enzymes: possible relevance to fluoropyrimidine chemotherapy. *Cancer Res.* **1993**, 53:2816–2822.

30 Lévi, F., Zidani, R., Vannetzel, J.M., Perpoint, B., Focan, C., Faggiuolo, R., Chollet, P., Garufi, C., Itzhaki, M., Dogliotti L.: Chronomodulated versus fixed-infusion-rate delivery of ambulatory chemotherapy with oxaliplatin, fluorouracil, and folinic acid (leucovorin) in patients with colorectal cancer metastases: a randomized multi-institutional trial. *J. Natl Cancer Inst.* **1994**, 86:1608–1617.

31 Lévi, F., Zidani, R., Misset, J.L.: Randomised multicentre trial of chronotherapy with oxaliplatin, fluorouracil, and folinic acid in metastatic colorectal cancer. *International Organization for Cancer Chronotherapy, Lancet* **1997**, 350:681–686.

32 Lévi, F., Focan, C., Karaboué, A., de la Valette, V., Focan-Henrard, D., Baron, B., Kreutz, M.F., Giacchetti, S.: Implications of circadian clocks for the rhythmic delivery of cancer therapeutics. *Adv. Drug Deliv. Rev.* **2007**, in press.

33 Altinok, A., Lévi, F., Goldbeter, A.: A cell cycle automaton model for probing circadian patterns of anticancer drug delivery. *Adv. Drug Deliv. Rev.* **2007**, doi: 10.1016/j.addr.2006.09.022.

34 Ermentrout, G. B., Edelstein-Keshet, L.: Cellular automata approaches to biological modeling. *J. Theor. Biol.* **1993**, 160:97–133.

35 Goldbeter, A.: Computational approaches to cellular rhythms. *Nature* **2002**, 420:238–245.

36 Blagosklonny, M. V., Pardee, A.B.: Exploiting cancer cell cycling for selective protection of normal cells (Review). *Cancer Res.* **2001**, 61:4301–4305.

37 Granda, T., Liu, X.H., Smaaland, R., Cermakian, N., Filipski, E., Sassone-Corsi, P., Lévi, F.: Circadian regulation of cell cycle and apoptosis proteins in mouse bone marrow and tumor. *FASEB J.* **2005**, 19:304–306.

38 You, S., Wood, P.A., Xiong, Y., Kobayashi, M., Du-Quiton, J., Hrushesky, W.J.: Daily coordination of cancer growth and circadian clock gene expression. *Breast Cancer Res. Treat.* **2005**, 91:47–60.

39 Iurisci, I., Filipski, E., Reinhardt, J., Bach, S., Gianella-Borradori, A., Iacobelli, S., Meijer, L., Lévi, F.: Improved tumor control through circadian clock induction by seliciclib, a cyclin-dependent kinase inhibitor. *Cancer Res.* **2007**, in press.

40 Yeh, K.T., Yang, M.Y., Liu, T.C., Chen, J.C., Chan, W.L., Lin, S.F., Chang, J.G.: Abnormal expression of period 1 (PER1) in endometrial carcinoma. *J. Pathol.* **2005**, 206:111–120.

41 Chen, S.T., Choo, K.B., Hou, M.F., Yeh, K.T., Kuo, S.J., Chang, J.G.: Deregulated expression of the PER1; PER2 and PER3 genes in breast cancers. *Carcinogenesis* **2005**, 26:1241–1246.

42 Gery, S., Gombart, A.F., Yi, W. S., Koeffler, C., Hofmann, W.K., Koeffler, H. P.: Transcription profiling of C/EBP targets identifies *Per2* as a gene implicated in myeloid leukaemia. *Blood* **2005**, 106:2827–2836.

43 Pogue-Geile, K.L., Lyons-Weiler, J., Whitcomb, D.C.: Molecular overlap of fly circadian rhythms and human pancreatic cancer. *Cancer Lett.* **2006**, 243:55–57.

44 Clairambault, J., Michel, P., Perthame, B.: Circadian rhythm and tumour growth *C.R. Acad. Sci. (Paris)* **2006**, 342:17–22.

45 Basdevant, C., Clairambault J., Lévi, F.: Optimisation of time-scheduled regimen for anti-cancer drug infusion. *Math. Mod. Numer. Anal.* **2005**, 39:1069–1086.

46 Dibrov, B.F., Zhabotinsky, A.M., Neyfakh, Y.A., Orlova, M.P., Churikova, L.I.: Mathematical model of cancer chemotherapy. Periodic schedules of phase-specific cytotoxic agent administration increasing the selectivity of therapy. *Math. Biosci.* **1985**, 73:1–31.

47 Dibrov, B.F.: Resonance effect in self-renewing tissues. *J. Theor. Biol.* **1998**, 192:15–33.

48 Agur, Z.: The effect of drug schedule on responsiveness to chemotherapy. *Ann. N.Y. Acad. Sci.* **1986**, 504:274–277.

49 Agur, Z., Arnon, R., Schechter, B.: Reduction of cytotoxicity to normal tissue by new regimens of cell-cycle phase-specific drugs. *Math. Biosci.* **1988**, 92:1–15.

50 Agur, Z., Arnon, R., Sandak, B., Schechter, B.: Zidovudine toxicity to murine bone marrow may be affected by the exact frequency of drug administration. *Exp. Hematol.* **1991**, 19:364–368.

51 Ubezio, P., Tagliabue, G., Schechter, B., Agur, Z.: Increasing 1-b-D-arabino-furanosylcytosine efficacy by scheduled dosing intervals based on direct measurements of bone marrow cell kinetics. *Cancer Res.* **1994**, 54:6446–6451.

52 Webb, G.F.: Resonance phenomena in cell population chemotherapy models. *Rocky Mountain J. Math.* **1990**, 20:1195–1216.

53 Andersen, L.K., Mackey, M.C.: Resonance in periodic chemotherapy: a case study of acute myelogenous leukemia. *J. Theor. Biol.* **2001**, 209:113–130.